Chapter 4
Point Defect Formation and Diffusion

The first step in understanding the effects of irradiation on materials is to understand, on the atomic level, the nature of radiation damage. In the previous chapters, we developed a quantitative description of the process of displacing an atom from its lattice site by the transfer of kinetic energy from a high-energy particle. The recoiling lattice atom travels through the crystal, colliding with its neighbors and displacing these also from their sites. A cascade of atomic collisions is created by the original particle with the end result being a number of vacant lattice sites and an equal number of displaced atoms wedged into the interstices of the lattice. The basic *defects* (vacancies and interstitials) form the foundation for *all* observed effects of irradiation on the physical and mechanical properties of materials. Determination of the concentration and diffusion of these basic defects is the subject of this chapter.

4.1 Properties of Irradiation-Induced Defects

Various types of defects exist in any crystalline lattice. These include the following:

- Point defects (0D): vacancies and interstitials
- Line defects (1D): dislocation lines
- Planar defects (2D): dislocation loops and
- Volume defects (3D): voids, bubbles, stacking-fault tetrahedra.

The most basic of these are point defects. Following [1], we will start with interstitials.

4.1.1 Interstitials

An interstitial is an atom that is located in a position of a crystal that is not a regular lattice site. There are two broad classifications of interstitial sites in the various

Additional material to this chapter can be downloaded from http://rmsbook2ed.engin.umich.edu/movies/

G.S. Was, *Fundamentals of Radiation Materials Science*,
DOI 10.1007/978-1-4939-3438-6_4

cubic crystal lattices: octahedral sites and tetrahedral sites, and these will be briefly reviewed. The fcc lattice is cubic with unit cell of length a (lattice constant) and with atoms located at the corners and the faces of the cube (Fig. 4.1). Each corner atom is shared by eight unit cells and each face atom is shared by two unit cells, so the number of atoms per unit cell is 8 corner atoms × 1/8 atom/unit cell + 6 face atoms × 1/2 atoms/unit cell = 4. Octahedral sites are interstitial positions that are surrounded by an octahedron where the lattice atoms make up the six vertices of an octahedron. There are four octahedral sites per unit cell in the fcc lattice, the center of the unit cell and the edges. The center site is wholly within the unit cell, but the sites on the edges are each shared by four unit cells (Fig. 4.2(a)). So the total number of octahedral interstitial sites per unit cell is 1 + 12 edge sites × 1/4 site per unit cell = 4 sites. There are also tetrahedral interstitial sites in the fcc lattice in which the atom is located inside a tetrahedron formed by lattice atoms. These are located inside the corners of the unit cell (Fig. 4.2(b)). There are a total of 8 tetrahedral sites (one for each corner) in the fcc unit cell.

In the bcc lattice, the atoms reside at the corners of the unit cell with one in the center of the cell for a total of two atoms per unit cell; 1 + 8 corner sites × 1/8 site/unit cell = 2 sites (Fig. 4.3). Octahedral interstitial sites are located on the faces and the edges of the unit cell giving 6 faces × 1/2 site per face +12 edges × 1/4 sites per edge = 6 sites per unit cell (Fig. 4.4(a)). Tetrahedral interstitial sites are located on the faces and in the corners of the faces. There are 6 faces × 4 locations per face × 1/2 sites/face = 12 tetrahedral sites (Fig. 4.4(b)).

The hcp unit cell is not cubic but rather hexagonal and is defined by the c/a ratio where a is the length of a side of the regular hexagon and c is the height of the cell (Fig. 4.5). There are six atoms per unit cell in the hcp lattice; twelve on the corners shared by six cells (=2) plus two on the faces shared by two cells (=1) plus three inside the cell at a height of $1/2c$ (=3). There are six octahedral sites per unit cell, all wholly contained within the unit cell (Fig. 4.6(a)). There are also six tetrahedral

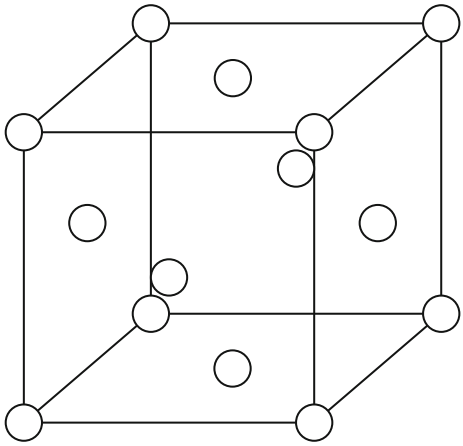

Fig. 4.1 Face-centered cubic (fcc) lattice unit cell

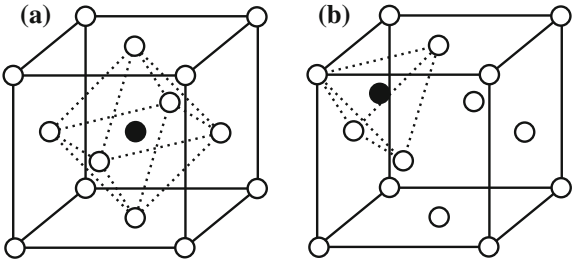

Fig. 4.2 Interstitial positions in the fcc unit cell, (**a**) octahedral site and (**b**) tetrahedral site

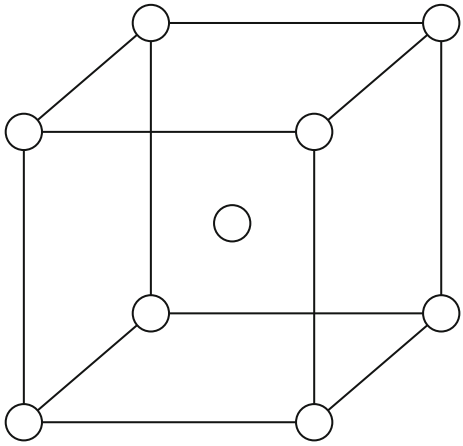

Fig. 4.3 Body-centered cubic (bcc) lattice unit cell

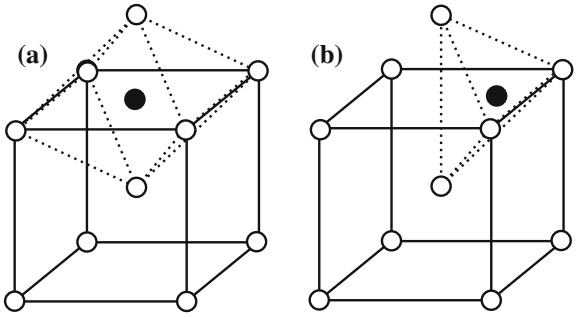

Fig. 4.4 Interstitial positions in the bcc unit cell, (**a**) octahedral site and (**b**) tetrahedral site

sites per unit cell, four wholly contained within the unit cell and six that are shared by each of three cells (Fig. 4.6(b)).

Our simple picture of interstitials is not a true physical picture because the stable configuration of self-interstitial atoms (SIA) in metals is the dumbbell or split-interstitial configuration where two atoms are associated with or "share" a single lattice site. Since the atom cores repel each other, the atoms arrange

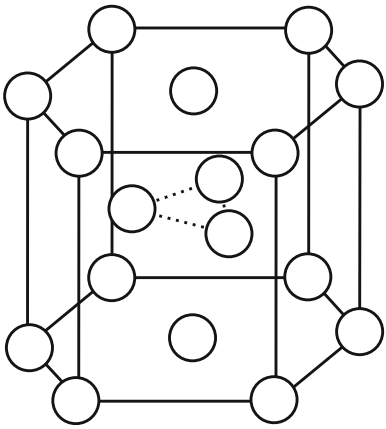

Fig. 4.5 Hexagonal close-packed (hcp) unit cell

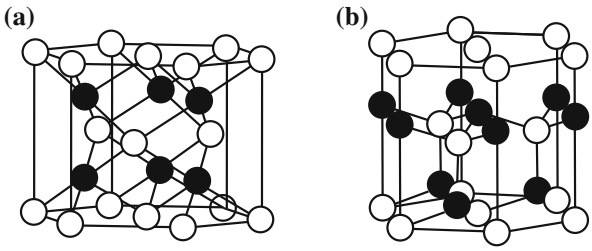

Fig. 4.6 Interstitial positions in the hcp unit cell (**a**) octahedral site and (**b**) tetrahedral site

themselves in the lowest energy orientation. This turns out to be with the dumbbell axis along the $\langle 100 \rangle$ direction for fcc metals, the $\langle 110 \rangle$ direction for bcc metals, and the $\langle 0001 \rangle$ direction for hcp crystals (Fig. 4.7).

To accommodate two atoms in one lattice site, atoms adjacent to the dumbbell are displaced slightly off their lattice positions which then perturbs neighboring atoms and so on. These displacements emanate from the defect, forming an elastic displacement field. The symmetry of the displacement field is reflected by the SIA configuration in the bcc lattice (Fig. 4.8).

Consider a $\langle 100 \rangle$ dumbbell interstitial configuration in fcc aluminum. The separation distance of the two dumbbells is about $0.6a$. The nearest neighbor spacing in the fcc lattice is along $\langle 110 \rangle$ and is $\left(a/\sqrt{2}\right)$, so the separation distance of a $\langle 100 \rangle$ dumbell is about 20 % smaller than the nearest neighbor distance in the undistorted lattice. The four nearest neighbors to each dumbbell are displaced outwards by about $0.1a$ and the total relaxation volume is about 2Ω, where Ω is the atomic volume. The relaxation volume is determined by treating the crystal as an

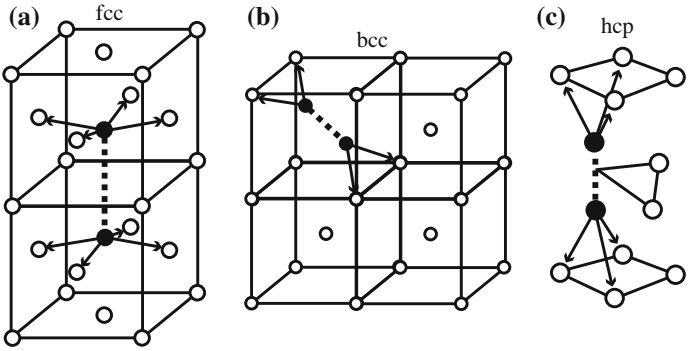

Fig. 4.7 Configurations of SIAs in (**a**) fcc, (**b**) bcc and (**c**) hcp lattices

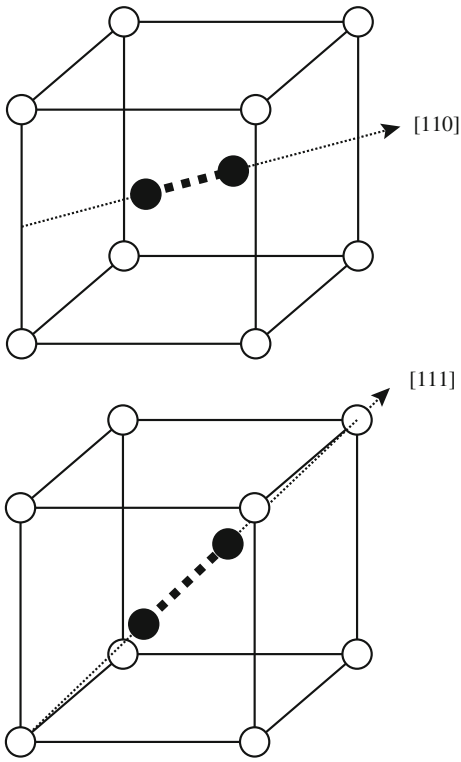

Fig. 4.8 Split interstitials in the bcc lattice

elastic continuum and inserting an atom as an interstitial (or removing one to create a vacancy) and determining the amount of distortion resulting in the lattice. The high relaxation volumes due to SIAs cause large lattice distortions, which lead to strong interaction with other SIAs and with other lattice defects (dislocation,

impurity atoms). The net effect of this elastic interaction is an attraction of mobile SIAs to these defects. Experimental values for the relaxation volume in several metals appear in Table 4.1.

4.1.2 Multiple Interstitials

Multiple interstitials form by the agglomeration of mobile SIAs at elevated temperatures. Multiple interstitials have a high binding energy on the order of 1 eV. Since the energy needed to dissociate a SIA from a large cluster approaches the SIA formation energy (2–4 eV), SIA clusters are very stable against dissociation at low temperatures.

Computer simulation predicts that the stable configuration of a di-interstitial in fcc metals is two parallel dumbbells on nearest neighbor sites (Fig. 4.9). The stable structure of tri-interstitials in fcc metals is predicted by computer simulation to be three orthogonal $\langle 100 \rangle$ dumbbells on nearest neighbor sites. The anticipated configuration of di-interstitials in the bcc lattice is two $\langle 110 \rangle$ dumbbells on nearest neighbor sites.

Table 4.1 Numerical values, compiled from different sources for some quantities characterizing properties of radiation-induced point defects in metals (from [1])

	Symbol	Unit	Al	Cu	Pt	Mo	W
Interstitials							
Relaxation volume	V^{i}_{relax}	Atomic vol.	1.9	1.4	2.0	1.1	
Formation energy	E^{i}_{f}	eV	3.2	2.2	3.5		
Equilibrium Concentration at T^{*}_{m}	$C_i(T_m)$	–	10^{-18}	10^{-7}	10^{-6}		
Migration energy	E^{i}_{m}	eV	0.12	0.12	0.06		0.054
Vacancies							
Relaxation volume	V^{v}_{relax}	Atomic vol.	0.05	–0.2	–0.4		
Formation energy	E^{v}_{f}	eV	0.66	1.27	1.51	3.2	3.8
Formation entropy	S^{v}_{f}	k	0.7	2.4			2
Equilibrium Concentration at T_m	$C_v(T_m)$	–	9×10^{-6}	2×10^{-6}			4×10^{-5}
Migration energy	E^{v}_{m}	eV	0.62	0.8	1.43	1.3	1.8
Activation energy for self-diffusion	Q_{vSD}	eV	1.28	2.07	2.9	4.5	5.7
Frenkel pairs							
Formation energy	E^{FP}_{f}	eV	3.9	3.5	5		

*Estimated by assuming $S^{f}_{i} = 8k$

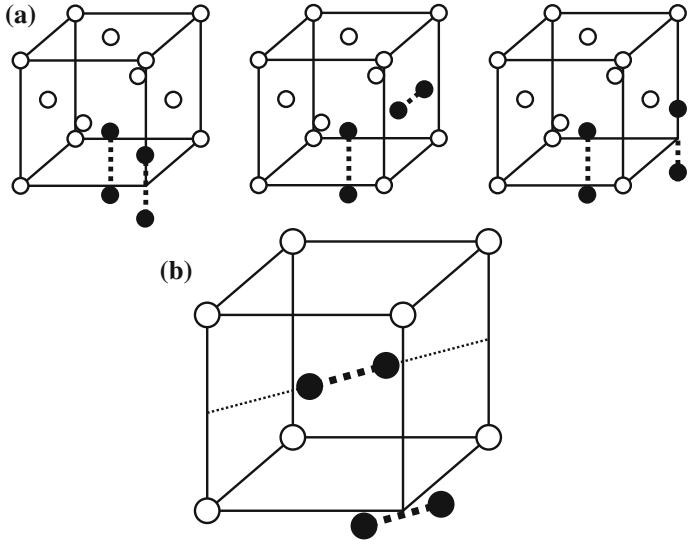

Fig. 4.9 Di-interstitials in the (**a**) fcc lattice in stable, metastable, and new stable positions and (**b**) in the bcc lattice

4.1.3 Interstitial–Impurity Complexes

Impurity atoms in metals are efficient traps for SIAs. Stable complexes consisting of undersized atoms and interstitials do not dissociate thermally below a temperature where vacancies become mobile. One possible configuration is the mixed dumbbell where one of the dumbbell atoms is replaced by the impurity atom (Fig. 4.10(a)). Binding energies are of the order of 0.5–1.0 eV. Weaker trapping is observed with oversized impurities (Fig. 4.10(b)).

Interstitial–impurity complexes require only a small activation energy to reorient themselves by so-called cage motion. Shown in Fig. 4.10(a), the impurity can jump between the indicated positions of the central octahedron, forming a new mixed dumbbell with the adjacent host atom. Since all of the mixed dumbbells have the impurity end toward the center of the cage, no long-range motion is associated with cage motion. The activation energy of the reorientation jump in the cage is about 0.01 eV.

Movies 4.1 and 4.2 (http://rmsbook2ed.engin.umich.edu/movies/) show the behavior of iron and chromium in an Fe–10 %Cr alloy following a displacement cascade as a function of the relative sizes of the solutes. In Movie 4.1, chromium is modeled as an oversized solute and in Movie 4.2 chromium is undersized. Note the difference in the interstitial clusters following the cascade cooling period. The undersize Cr in Movie 4.2 undergoes stronger trapping by the iron interstitials than

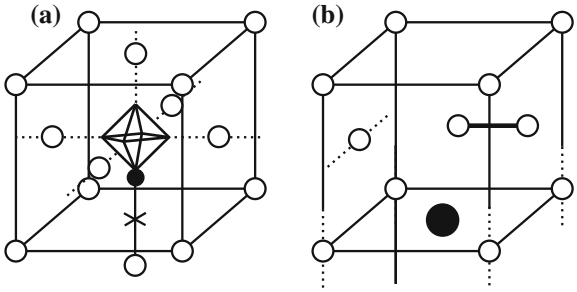

Fig. 4.10 (**a**) Mixed dumbbell configuration in the fcc lattice formed by an undersized impurity and an atom of the host lattice. The vertices of the octahedron are the other locations of the impurity as it makes a dumbbell with the other "face" atoms in the unit cell. (**b**) Trapping of an interstitial to make a dumbbell with an oversized impurity in the fcc lattice

in the case of oversize Cr in Movie 4.1, resulting is a greater number of small interstitial clusters containing Cr.

4.1.4 Vacancies

The vacancy, or missing lattice atom, is the simplest point defect in metal lattices. All calculations and computer simulations show that the single vacancy structure is a missing lattice atom with the nearest neighbors relaxing inward toward the vacancy.

SIAs have a high formation energy (>2.0 eV), a large relaxation volume ($\sim 2\Omega$) and a low migration energy (<0.15 eV) leading to a high mobility. Vacancies, on the other hand, have low formation energies (<2 eV), low relaxation volume (0.1–0.5Ω), and high migration energy (>0.5 eV) and are therefore much less mobile than SIAs (Table 4.1). Further, the strain field of vacancies is isotropic in cubic metals making them hard to investigate.

4.1.5 Multiple Vacancies

Multiple vacancies have small binding energies compared to interstitial clusters (0.1 eV) but are often observed in irradiated metals. The configuration of multiple vacancy clusters is shown for the fcc lattice in Fig. 4.11(a), and for the bcc lattice in Fig. 4.11(b). The migration energy of divacancies is less than for single vacancies (0.9 eV vs. 1.32 eV for Ni) but increases with increasing cluster size. It appears that since the tetra-vacancy can only migrate by dissociation, it is the first stable nucleus for further clustering.

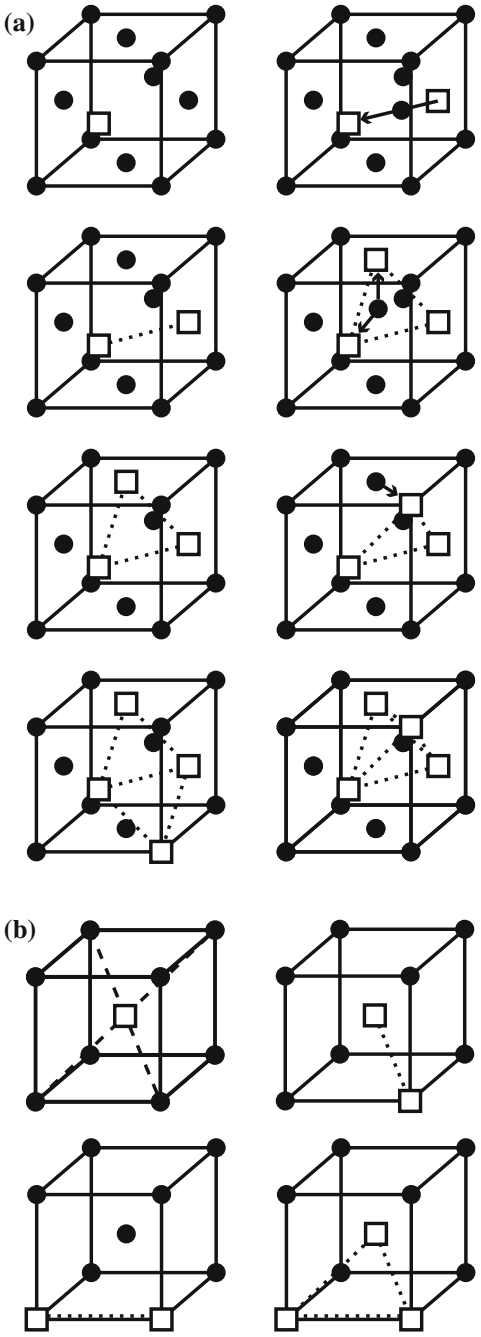

Fig. 4.11 Configurations of multiple vacancies in the (**a**) fcc lattice and (**b**) bcc lattice

4.1.6 Solute–Defect and Impurity–Defect Clusters

Vacancies can bind to oversize solute or oversize impurity atoms in order to lower the overall free energy of the solid. Estimates of the binding energy of a vacancy to an oversize solute in the fcc lattice range from 0.2 to 1.0 eV [2]. Hence, these solutes can act as efficient traps for vacancies in the lattice.

4.2 Thermodynamics of Point Defect Formation

Even in the absence of irradiation, a crystal cannot exist at a finite temperature in a state of absolute perfection. Statistically, there is a finite probability that sufficient energy will be concentrated, by local fluctuations, to form a defect in the crystal lattice. For most purposes, it is fair to assume that the volume of the crystal is constant, for which the Helmholtz free energy function applies. Following [3], if the system is at constant pressure, then:

$$F \cong G = U + pV - TS = H - TS, \tag{4.1}$$

where U is the internal energy, H is the total enthalpy of the N atoms comprising the system, S represents the disorder (entropy) in the system which can be characterized by:

$$S = k \ln w, \tag{4.2}$$

where w is the number of possible different configurations of atoms and k is Boltzmann's constant.

Suppose that a crystal has n defects with N available sites. The increase in free energy is:

$$\Delta G_{\mathrm{f}} = n\Delta H_{\mathrm{f}} - T\Delta S, \tag{4.3}$$

where ΔH_{f} is the increase in enthalpy brought about by the introduction (formation) of the defect and ΔS is the change in total entropy, determined as follows.

For one defect, there are N available sites and hence N possible configurations. For n defects, there are N for the first, $(N - 1)$ for the second, $(N - 2)$ for the third, etc., up to $(N - n + 1)$ for the nth. This leads to $N(N - 1)(N - 2)\ldots(N - n + 1)$ configurations in all. But because these are not all distinct and defects are indistinguishable, the number above allows for $n!$ ways of distributing N defects among n sites. Hence, the number of possible different configurations is:

$$w = \frac{N(N-1)(N-2)\ldots(N-n+1)}{n!}, \tag{4.4}$$

or

$$w = \frac{N!}{n!(N-n)!}. \tag{4.5}$$

The *mixing entropy* is then:

$$\Delta S_{\text{mix}} = k[\ln N! - \ln n! - \ln (N-n)!]. \tag{4.6}$$

Using Stirling's approximation of $\ln x! \simeq x \ln x$ for large x gives:

$$\Delta S_{\text{mix}} = k \ln w \cong k[N \ln N - n \ln n - (N-n) \ln (N-n)]. \tag{4.7}$$

In addition to ΔS_{mix}, there is a contribution to ΔS from the vibrational disorder of the presence of the defects. According to the Einstein model of lattice motion, the atoms are represented as $3N$ independent linear harmonic oscillators and the associated entropy is:

$$S_{\text{f}} = 3k \ln\left(\frac{kT}{\hbar \nu_{\text{E}}}\right), \tag{4.8}$$

where ν_{E} is the natural frequency of the oscillator and $\hbar$ is Planck's constant. If each defect changes the vibration frequency of z neighbors to ν_{r}, the entropy is:

$$S'_{\text{f}} = 3kz \ln\left(\frac{kT}{\hbar \nu_{\text{r}}}\right) = 3kz\left[\ln\left(\frac{kT}{\hbar \nu_{\text{E}}}\right) + \ln\left(\frac{\nu_{\text{E}}}{\nu_{\text{r}}}\right)\right], \tag{4.9}$$

and for n defects, the total change in entropy due to vibrational disorder is:

$$n\left(S'_{\text{f}} - zS_{\text{f}}\right) = \Delta S_{\text{f}} = 3nkz \ln\left(\frac{\nu_{\text{E}}}{\nu_{\text{r}}}\right). \tag{4.10}$$

Taking both contributions to the entropy change and inserting them into the free energy equation gives:

$$\Delta G_{\text{f}} = n\Delta H_{\text{f}} - kT\left[N \ln N - n \ln n - (N-n)\ln(N-n) + n \ln\left(\frac{\nu_{\text{E}}}{\nu_{\text{r}}}\right)^{3z}\right]. \tag{4.11}$$

In equilibrium, n will be such that it satisfies $\mathrm{d}\Delta G_{\text{f}}/\mathrm{d}n = 0$ giving:

$$\frac{\Delta H_{\text{f}}}{kT} = \ln\left[\frac{N-n}{n}\left(\frac{\nu_{\text{E}}}{\nu_{\text{r}}}\right)^{3z}\right]. \tag{4.12}$$

Assuming $n \ll N$ and letting $n/N = C$ (concentration fraction):

$$C = \left(\frac{\nu_E}{\nu_r}\right)^{3z} \exp\left(\frac{-\Delta H_f}{kT}\right). \tag{4.13}$$

Writing $\left(\frac{\nu_E}{\nu_r}\right)^{3z}$ in terms of entropy gives the familiar equation:

$$C = \frac{n}{N} = \exp\frac{\Delta S_f}{k} \exp\frac{-\Delta H_f}{kT} = \exp\left(\frac{-\Delta G_f}{kT}\right). \tag{4.14}$$

For vacancies, we have

$$C_v = \exp\left(\frac{S_f^v}{k}\right) \exp\left(\frac{-E_f^v}{kT}\right), \tag{4.15}$$

and for interstitials:

$$C_i = \exp\left(\frac{S_f^i}{k}\right) \exp\left(\frac{-E_f^i}{kT}\right), \tag{4.16}$$

where $E_f^v = \Delta H_f^v$ and $E_f^i = \Delta H_f^i$ are the formation energies for the respective defect type, and $\Delta S_f^v = S_f^v, \Delta S_f^i = S_f^i$. In metals, typical values for E_f^v are ~ 1 eV, and for $E_f^i \sim 4$ eV. Hence, the formation of vacancies requires considerably less energy than the formation of interstitials (see Table 4.1) and so at thermal equilibrium, $C_v \gg C_i$. Let us look at an example.

Example 4.1 Calculate the equilibrium concentration of vacancies and interstitials in aluminum at room temperature and 10 °C below the melting point.

(a) $RT \simeq 20$ °C or 293 K
From Table 4.1, we have

$$E_f^v \cong 0.66 \text{ eV} \quad S_f^v \sim 0.7k$$
$$E_f^i \cong 3.2 \text{ eV} \quad S_f^i \sim 8k,$$

and inserting into Eqs. (4.15) and (4.16) yields

$$C_v = \exp\left(S_f^v/k\right) \exp\left(-E_f^v/kT\right) \sim 1.6 \times 10^{-11}$$
$$C_i = \exp\left(S_f^i/k\right) \exp\left(-E_f^i/kT\right) \sim 5.0 \times 10^{-51}.$$

(b) At 10 °C below T_m or 650 °C (923 K)
Equations (4.15) and (4.16) yield

$$C_v = \exp\left(S_f^v/k\right)\exp\left(-E_f^v/kT\right) \sim 5.0 \times 10^{-4}$$
$$C_i = \exp\left(S_f^i/k\right)\exp\left(-E_f^i/kT\right) \sim 9.8 \times 10^{-15}.$$

Besides doing an experiment, how do we go about obtaining an estimate for E_f^v? Suppose we create a small cavity in a rigid crystal that has a volume $\Omega = 4/3\pi r_a^3$ equal to the volume occupied by one atom, where Ω is the atom volume and r_a is the atom radius. Since we must conserve volume, we spread the material from the cavity uniformly over the surface of a crystal. If the crystal is a sphere, we have:

$$R' = R + \Delta R. \tag{4.17}$$

Since the crystal is a rigid medium and volume is conserved:

$$4\pi R^2 \Delta R = 4/3\pi r_a^3, \tag{4.18}$$

and if the crystal is large compared to the size of the atom, then $R \gg r_a$ and $\Delta R \ll R$ and:

$$\Delta R = r_a^3/3R^2. \tag{4.19}$$

If E_f^v is the difference in surface energy of the crystal with and without a cavity and σ is the surface energy per unit area, then:

$$\begin{aligned} E_f^v &= 4\pi r_a^2\sigma + 4\pi\sigma(R+\Delta R)^2 - 4\pi R^2\sigma \\ &\sim 4\pi\sigma\left(r_a^2 + 2R\Delta R\right), \end{aligned} \tag{4.20}$$

where the first two terms on the right-hand side of the equation are the energies associated with the inner and outer surfaces after formation of the vacancy and the last term is the energy of the surface of the crystal before formation of the vacancy, and the ΔR^2 term has been neglected. Substituting for ΔR from Eq. (4.19) gives:

$$\begin{aligned} E_f^v &= 4\pi\sigma\left(r_a^2 + \frac{2}{3}\frac{r_a^3}{R}\right) \\ &= 4\pi\sigma r_a^2\left(1 + \frac{2}{3}\frac{r_a}{R}\right), \end{aligned} \tag{4.21}$$

and since $r_a \ll R$, we have:

$$E_f^v \sim 4\pi\sigma r_a^2. \tag{4.22}$$

In most metals, $\sigma \sim 10$ eV/nm^2 and $r_a \sim 0.15$ nm, so $E_f^v \sim 2$ eV.

If we treat the crystal as an elastic continuum, we get a different expression for E_f^v:

$$E_f^v = 4\pi r_a^2 \sigma - 12\pi r_a \frac{\sigma^2}{\mu} + 6\pi r_a \frac{\sigma^2}{\mu}, \tag{4.23}$$

where the first term is the surface energy of the cavity, the second term is the reduction in surface energy due to contraction of the surface by the surface tension, and the third term is the elastic energy stored in the solid, μ is the shear modulus of the crystal, and $E_f^v \sim 1\,\text{eV}$. Note that an interstitial will cause a displacement that is greater than r_a, resulting in a greater formation energy as we have seen already.

4.3 Diffusion of Point Defects

Atoms in a lattice are in a constant state of motion due to thermal vibration, and this means that point defects in the lattice are also in motion. The random nature of thermal vibration gives rise to random walk of the atoms via the defects that are in thermal equilibrium with their surroundings, known as *self-diffusion*. If foreign atoms are present in a pure metal, their diffusion is known as *heterodiffusion*. Self-diffusion arises when a local concentration gradient of defects appears in the crystal, driving atoms to move in the direction that eliminates the gradient. Diffusion is driven by forces other than the concentration gradient, such as stress or strain, electric fields, temperature, etc. In the most general sense, diffusion is driven by a difference in chemical potential. Diffusion in a polycrystal is a complex mechanism due to the presence of grain boundaries, internal surfaces, dislocations, etc. We will follow the analysis in [4] by starting with diffusion in a single crystal and then expanding our treatment to include the polycrystalline case later on.

4.3.1 Macroscopic Description of Diffusion

Diffusion is governed by two fundamental laws derived by Fick in 1880. They apply to any state of matter due to their general character regarding macroscopic diffusion processes. The first law is a relationship between the flux, J, and the concentration gradient of the diffusing specie:

$$J = -D\nabla C, \tag{4.24}$$

where D is the diffusion coefficient and ∇C is the composition gradient. For diffusion in one-dimension,

$$J = -D\frac{\partial C}{\partial x}. \tag{4.25}$$

The minus sign indicates that diffusion takes place in the direction of *decreasing* concentration of the diffusing specie. D is generally given in units of cm^2/s or m^2/s and for solids between 20 and 1500 °C, 10^{-20} $cm^2/s < D < 10^{-4}$ cm^2/s.

Fick's second law gives a relation between the concentration gradient and the rate of change of concentration caused by diffusion at a given point in the system:

$$\frac{\partial C}{\partial t} = -\nabla \cdot J = -\nabla \cdot D\nabla C,$$

which, in one-dimension simplifies to:

$$\frac{\partial C}{\partial t} = -\frac{\partial}{\partial x}\left(D\frac{\partial C}{\partial x}\right). \tag{4.26}$$

If D is not a function of the concentration, then we can write Eq. (4.26) as:

$$\begin{aligned}\frac{\partial C}{\partial t} &= -D\nabla^2 C \\ &= -D\frac{\partial^2 C}{\partial x^2}.\end{aligned} \tag{4.27}$$

Equations (4.26) or (4.27) can be solved for certain limiting conditions enabling D to be determined on the basis of various measurements.

While Fick's laws provide a description of diffusion on the macroscopic scale, we would like to understand diffusion on the microscopic level as well. Diffusion occurs by several possible mechanisms depending on the nature of the diffusing specie and the host lattice. We will examine these mechanisms and then derive a description of diffusion on the microscopic level.

4.3.2 Mechanisms of Diffusion

To obtain a theoretical description of diffusion, we first consider the elementary act of a jump of an atom from one stable position to another in the lattice. There are several mechanisms of lattice diffusion, some requiring the presence of defects, others not. The following types [5] can be distinguished.

Exchange and ring mechanisms: The exchange mechanism (Fig. 4.12) consists of the exchange of lattice positions involving two atoms located in adjacent crystal sites. It does not require the presence of defects, and it is highly improbable in close-packed crystals since it requires considerable deformation and hence an enormous activation energy. The ring mechanism (Fig. 4.13) is less energy

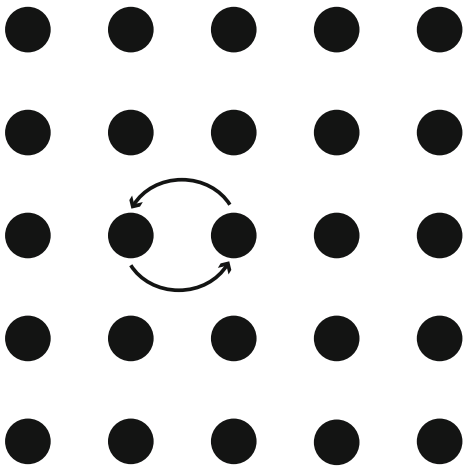

Fig. 4.12 Exchange mechanism of diffusion

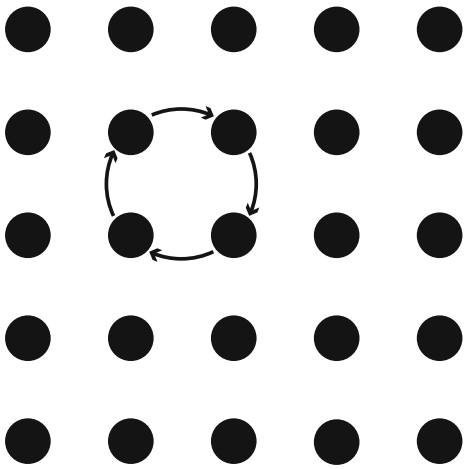

Fig. 4.13 Ring mechanism of diffusion

intensive but requires the coordinated movement of three to five atoms. Since the probability of this is low and the energy required is still high, both the exchange and ring mechanisms are unimportant in crystals containing defects.

Vacancy mechanism: This is the simplest mechanism of diffusion and occurs in metals and alloys (Fig. 4.14). Diffusion occurs by the jump of an atom from its lattice site to a vacant site. For an atom to move by this mechanism, the presence of a neighboring vacancy is required. Since movement of the vacancy is opposite that of the atom, vacancy-type diffusion is regarded as either a movement of the atom or the equivalent movement of the vacancy. However, as we will see, the diffusion coefficient for vacancy diffusion is *not* equal to that for atom diffusion.

Interstitial mechanism: This mechanism involves the movement of an atom from one interstitial position to another (Fig. 4.15). It requires considerable energy in

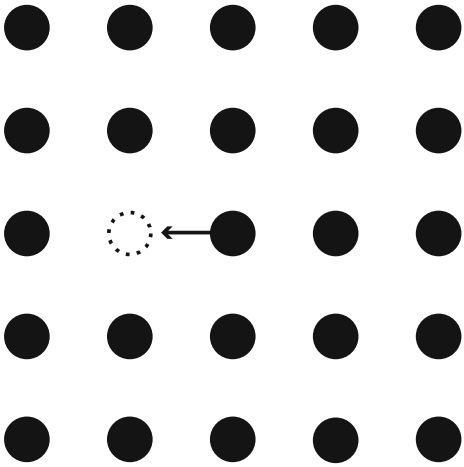

Fig. 4.14 Vacancy mechanism of diffusion

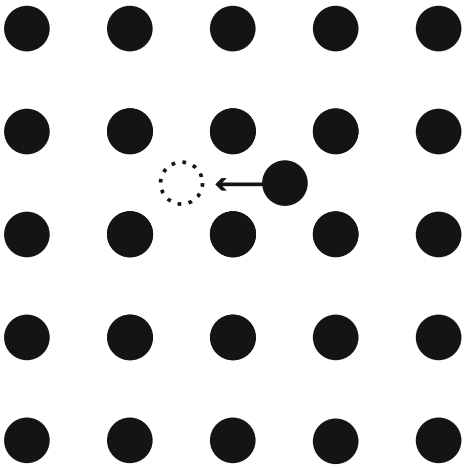

Fig. 4.15 Interstitial mechanism of diffusion

order to push its way through the barrier atoms separating the interstitial sites in the crystal (recall the role of barrier atoms in our calculation of displacement energy in Chap. 2). In reality, this mechanism only occurs when the diffusing species is of an atom type that is smaller than the host lattice atoms.

Interstitialcy mechanism: This mechanism involves the displacement of nearby lattice atoms to an interstitial site and generally occurs when atom diameters are comparable. There are two variants of this mechanism: the collinear variant in which displaced atoms move along a straight line (Fig. 4.16(a)) and the non-collinear variant in which the displaced atom moves to the interstitial position at an angle to the direction of movement of the displacing atom (Fig. 4.16(b)).

Dumbbell interstitial mechanism: This process involves the symmetrical placement of an interstitial and a lattice atom about a single lattice site such that they

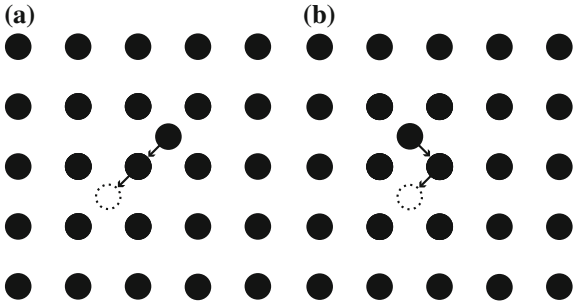

Fig. 4.16 Interstitialcy mechanism of diffusion (**a**) collinear variant and (**b**) non-collinear variant

share the lattice site. Figure 4.17 shows a 2D schematic of the sharing of a single lattice site by two atoms. Recall from our discussion in Sect. 4.1 that the dumbbell is a very stable configuration for the interstitial and that there are preferred directions for the dumbbell that depend on the lattice, and minimize the energy.

Crowding (*crowdion*) *mechanism*: This mechanism occurs when an atom is added to a lattice plane, but it does not reside in an interstitial position. To accommodate the atom, lattice atoms over, perhaps, 10 lattice constants are all shifted with respect to their lattice sites. The configuration can be thought of as a dumbbell spread over 10 atoms along a row, rather than two (Fig. 4.18). Actually, we have already seen a crowdion in our discussion of focusing collisions. Re-examine Fig. 3.4 and you will see a crowdion emanating from the displacement spike. This configuration is not a stable configuration and exists only temporarily as the energy for the knock-on atoms is expended.

Despite the numerous mechanisms for diffusion of atoms in a solid, diffusion usually occurs by either the vacancy or interstitialcy mechanisms. Ultimately, we want to obtain a mathematical relation between the macroscopic parameters for diffusion (i.e., the self-diffusion coefficient) and the elementary acts of defect jumps represented by the coefficients of diffusion for defects, or the microscopic process. We will assume that the self-diffusion process consists of a completely random walk of defects, i.e., there is no correlation between successive jumps of the defects.

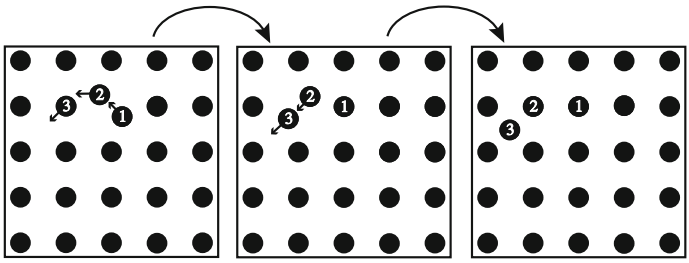

Fig. 4.17 Dumbbell interstitial mechanism of diffusion

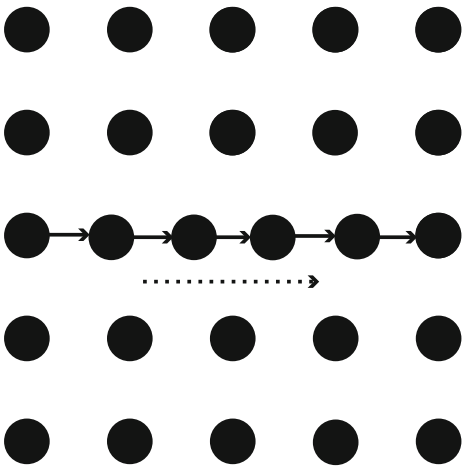

Fig. 4.18 Crowdion mechanism of diffusion

Although this is reasonable for defect diffusion, it is not strictly true for atom diffusion. As mentioned earlier, jumps of defects and hence, atoms, are due to thermal vibrations of very high frequency. The Debye frequency is $\sim 10^{13}\ \mathrm{s}^{-1}$. The frequency of atom jumps is orders of magnitude lower, $\sim 10^{8}\ \mathrm{s}^{-1}$ at say, 700 °C. This means that once every 10^5 vibrations, a thermal fluctuation is large enough for an atom to overcome the energy barrier separating it from the next stable position. Let us take a closer look at the jumping process.

4.3.3 Microscopic Description of Diffusion

Suppose that at time zero, a single impurity atom is placed in a position in a crystal which is designated as the origin. The atom proceeds to jump from one site to another in a completely random manner. Each jump is of distance λ, but since the medium is assumed to be isotropic, each jump is arbitrary and independent of previous jumps. After a time t, the displacement, r, of the particle from the origin is measured. If the experiment is repeated several times, r will not be the same because of the stochastic nature of the process. Rather, the displacements will be distributed according to a function $P_t(r)$ where $P_t d^3 r$ is the probability of finding the atom in a volume element $d^3 r$ a distance r from the origin after time t. The quantity that best describes the extent of migration is the mean square displacement, $\overline{r^2}$, which is given by the second moment of the distribution:

$$\overline{r^2} = \int_{\text{all space}} r^2 P_t(r) d^3 r = 4\pi \int_0^\infty r^4 P_t(r) dr. \tag{4.28}$$

We will first compute $\overline{r^2}$ without knowledge of $P_t(r)$.

If the atom makes Γ jumps per unit time, the time interval t corresponds to a number of n jumps given by:

$$n = \Gamma t. \tag{4.29}$$

Each jump is represented by a vector $\underline{\lambda_i}$, where the subscript, i, refers to the jump number. The vectors are all of the same length, λ_i, but of random direction. The position of the diffusing atom after n jumps (Fig. 4.19) is the vector sum of the $\underline{\lambda_i}$ or:

$$\underline{r} = \underline{\lambda}_1 + \underline{\lambda}_2 + \underline{\lambda}_3 \ldots + \underline{\lambda}_n. \tag{4.30}$$

The magnitude of the square of the displacement is obtained by taking the scalar product of $\underline{r}$ with itself:

$$r^2 = \underline{r} \cdot \underline{r} = (\underline{\lambda}_1 + \underline{\lambda}_2 + \underline{\lambda}_3 \ldots + \underline{\lambda}_n) \cdot (\underline{\lambda}_1 + \underline{\lambda}_2 + \underline{\lambda}_3 \ldots + \underline{\lambda}_n). \tag{4.31}$$

The scalar product of two sums is equivalent to squaring the sums, giving:

$$r^2 = \sum_{i=1}^{n} \underline{\lambda}_i \cdot \underline{\lambda}_i + 2 \sum_{i=1}^{n-1} \sum_{j \neq i}^{n} \underline{\lambda}_i \cdot \underline{\lambda}_j. \tag{4.32}$$

The first term is equal to $n\lambda^2$ and the second term can be rewritten as:

$$\underline{\lambda}_i \cdot \underline{\lambda}_j = \lambda^2 \cos \theta_{ij}, \tag{4.33}$$

and

$$r^2 = n\lambda^2 + 2\lambda^2 \sum_{i=1}^{n-1} \sum_{j \neq i}^{n} \cos \theta_{ij}, \tag{4.34}$$

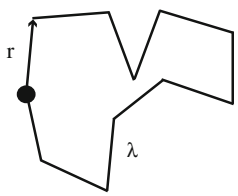

Fig. 4.19 Random jump of a defect in an isotropic solid

or

$$r^2 = n\lambda^2\left(1 + \frac{2}{n}\sum_{i=1}^{n-1}\sum_{j\neq i}^{n}\cos\theta_{ij}\right). \tag{4.35}$$

The mean square displacement is obtained by averaging r^2 over a large number of experiments. The term $\cos\theta_{ij}$ can range from -1 to 1, and by nature of the random hopping process, the average value of $\cos\theta_{ij}$ for any $i\,j$ combination is zero. Hence, the last term disappears and:

$$\overline{r^2} = n\lambda^2, \tag{4.36}$$

or

$$\overline{r^2} = \lambda^2 \Gamma t. \tag{4.37}$$

Equation (4.37) relates the mean square displacement to the microscopic properties of jump distance and jump frequency. Now, we wish to compute $\overline{r^2}$ from a macroscopic viewpoint.

At $t = 0$, N impurity atoms are introduced into a restricted region of a host crystal. As a consequence of diffusion (random hopping), the N atoms spread out from the origin in a manner described by $C(r, t)$ which is obtained by solving Fick's second law (assuming D is not a function of concentration):

$$\frac{\partial C}{\partial t} = D\frac{1}{r^2}\frac{\partial}{\partial r}\left(r^2\frac{\partial C}{\partial r}\right), \tag{4.38}$$

with initial condition $C(r, 0) = 0$, for $r \neq 0$. Since the N atoms remain in the crystal, $C(r, t)$ is subject to the constraint:

$$\int_0^\infty 4\pi r^2 C(r,t)\mathrm{d}r = N, \tag{4.39}$$

with boundary condition that the concentration drops to 0 at infinity, $C(\infty, t) = 0$. The solution to Eq. (4.38) subject to the initial and boundary conditions becomes:

$$C(r,t) = N\frac{\exp(-r^2/4Dt)}{(4\pi Dt)^{3/2}}. \tag{4.40}$$

The probability of finding the single atom in a spherical shell between r and $r + \mathrm{d}r$ after time t is equivalent (in the macroscopic diffusion description of the

problem) to the fraction of the N atoms located in the same volume element after time t. $P_r(r)$ and $C(r, t)$ are related by:

$$P_t(r) = \frac{C(r,t)}{N} = \frac{\exp(-r^2/4Dt)}{(4\pi Dt)^{3/2}}. \tag{4.41}$$

The mean square displacement is:

$$\begin{aligned} \overline{r^2} &= 4\pi \int_0^\infty r^4 P_t(r) \mathrm{d}r \\ &= \frac{4\pi}{(4\pi Dt)^{3/2}} \int_0^\infty r^4 \exp\left(-r^2/4Dt\right) \mathrm{d}r, \end{aligned} \tag{4.42}$$

or

$$\overline{r^2} = 6Dt. \tag{4.43}$$

Comparing to $\overline{r^2} = \lambda^2 \Gamma t$ from our microscopic solution Eq. (4.37), we have:

$$D = \frac{1}{6}\lambda^2 \Gamma \tag{4.44}$$

which is the Einstein formula and is the link between the microscopic diffusion parameters λ and Γ, and the macroscopic diffusion parameter, D.

4.3.4 Jump Frequency, Γ

We define Γ as the total number of jumps per second for an atom. Therefore, in a time increment δt, we expect $\Gamma \delta t$ jumps. The quantity $\Gamma \delta t$ is proportional to z, the number of nearest neighbors (sites), p_v, the probability that a given neighboring site is vacant, and ω, the frequency with which an atom jumps to a particular site. Thus, the frequency with which an atom jumps to any neighboring equilibrium site, Γ, is the product of the jump frequency to a single site, ω, the number of nearest neighbor sites, z, and the probability that one site is vacant, p_v or:

$$\Gamma = z p_v \omega, \tag{4.45}$$

and

$$D_{\mathrm{a}}^{\mathrm{v}} = \frac{1}{6} z \lambda^2 p_{\mathrm{v}} \omega, \tag{4.46}$$

where we have properly included the subscript, a and superscript, v to indicate that this is the diffusion coefficient for *atom diffusion* via vacancies. Also note that the jump distance λ is related to the lattice constant by $\lambda = Aa$, where the coefficient, A, depends on the diffusion mechanism and the crystal structure. The terms $\frac{1}{6} z A^2$ are often lumped together into a single parameter, α, such that:

$$D_{\mathrm{a}}^{\mathrm{v}} = \alpha a^2 p_{\mathrm{v}} \omega, \tag{4.47}$$

and if vacancy motion is random, then $p_{\mathrm{v}} = N_{\mathrm{v}}$ and:

$$D_{\mathrm{a}}^{\mathrm{v}} = \alpha a^2 N_{\mathrm{v}} \omega. \tag{4.48}$$

Let us look at an example of how to determine α for a specific diffusion process and crystal structure.

Example 4.2. Vacancy diffusion in the bcc and fcc lattices
In the case of the vacancy mechanism of diffusion in a bcc structure, each atom has eight nearest neighbors ($z = 8$). The jump distance is related to a by $A = \frac{\sqrt{3}}{2}$, and hence, $\alpha = 1$. For the simple interstitial diffusion mechanism in a bcc lattice, $z = 4$ and $A = \frac{1}{2}$ giving $\alpha = \frac{1}{6}$.

For the fcc lattice, $z = 12$ and $A = \frac{1}{\sqrt{2}}$, giving $\alpha = 1$. For interstitials in the fcc lattice, $z = 12$ and $A = \frac{1}{2}$, and $\alpha = \frac{1}{2}$.

Before continuing, it is instructive to point out the difference between vacancy diffusion and atom diffusion via a vacancy mechanism (vacancy self-diffusion). In determining the components of Γ, we noted that Γ depends on the probability, p_{v}, that a neighboring lattice site is vacant. This is a necessary condition for an atom jump via a vacancy. However, if we are following the migration of the vacancy, then Γ depends on the probability that a neighboring lattice site to the vacancy is filled by an atom. Since in all but the most extreme cases this probability is ~1, and the equation for vacancy diffusion is given as follows:

$$D_{\mathrm{v}} = \alpha a^2 \omega, \tag{4.49}$$

and differs from that for vacancy self-diffusion by the factor N_{v}.

4.3.5 *Jump Frequency, ω*

In calculating ω, we will ignore detailed atomic movements and instead deal in terms of "activated complexes" or regions containing an atom midway between two equilibrium sites (Fig. 4.20). The number of atoms diffusing per second is then obtained by multiplying the number of activated complexes (n_m) by the average velocity of the atoms moving through this barrier ($\bar{\upsilon}$) divided by the width of the barrier (δ). The jump frequency is then:

$$\omega = \frac{N_m \bar{\upsilon}}{\delta}, \tag{4.50}$$

where N_m is the mole fraction of activated complexes. The work done in moving an atom across this barrier is equal to the change in Gibbs free energy for the region, ΔG_m:

$$\Delta G_m = \Delta H_m - T\Delta S_m. \tag{4.51}$$

Using ΔG_m, the equilibrium mole fraction of atoms in the region of the saddle point in Fig. 4.20, N_m can be calculated; in the same way, we calculated N_v. Instead of mixing vacancies to raise the free energy by ΔG_v per mole, we are mixing complexes to raise the free energy an amount ΔG_m per mole. The ideal entropy of mixing is the same for vacancies as for complexes so, at equilibrium, n_m out of N atoms will be in the neighborhood of the saddle point at any instant and:

$$\frac{n_m}{N} = N_m = \exp\left(\frac{-\Delta H_m + T\Delta S_m}{kT}\right) = \exp\left(\frac{-\Delta G_m}{kT}\right). \tag{4.52}$$

From Eq. (4.50), $\omega = \frac{N_m \bar{\upsilon}}{\delta}$ and $\bar{\upsilon}/\delta$ is the frequency (call it ν) at which atoms at the saddle point jump to the new site. Thus, $n_m\nu$ out of N atoms will jump from one site to a given site per second, and the average jump frequency is:

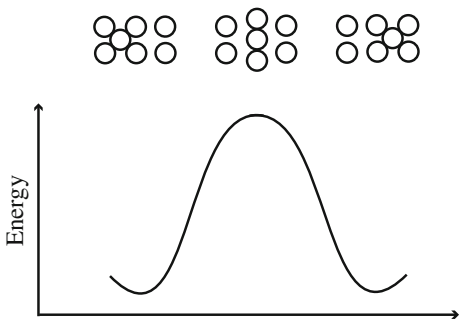

Fig. 4.20 Passage of the "activated complex" from one stable position, through a saddle point, to another stable position

$$\frac{n_m v}{N} = \omega = v \exp\left(\frac{-\Delta G_m}{kT}\right) = v \exp\left(\frac{-\Delta S_m}{k}\right) \exp\left(\frac{-\Delta H_m}{kT}\right)$$
$$= v \exp\left(\frac{S_m}{k}\right) \exp\left(\frac{-E_m}{kT}\right), \tag{4.53}$$

where v is the Debye frequency ($\sim 10^{13}$ s^{-1}) and $E_m = \Delta H_m$ and $S_m = \Delta S_m$.

A more precise treatment considers the fact that not all jump directions are equal and that inequality is reflected in the frequency. So-called multifrequency models are used to describe diffusion in dilute alloys [6]. For vacancy-atom jumps in fcc alloys, there are five frequencies of interest, as shown in Fig. 4.21. The solute atom, shown as shaded, will exchange with the vacancy with a jump frequency ω_2. Near to the solute atom, solvent atoms may have jump frequencies that are different from the value ω_0 characteristic of pure solvent. ω_1 is the frequency for solvent-vacancy jumps between a pair of sites that are both nearest neighbors of a solute. ω_3 is for vacancy jumps from first to more distant neighbor sites (second, third, or fourth) and are referred to as dissociative jumps. Finally, ω_4 is the frequency for the reverse, or associative jumps onto first neighbor sites. All other solvent-vacancy jumps are assumed to occur with the frequency ω_0. Thus, each jump frequency, ω_j, will have an Arrhenius-type temperature dependence with activation enthalpy, H_j, and pre-exponential factor, v_j, yielding equations of the form:

$$\omega_j = v_j \exp\left(\frac{-H_j}{kT}\right). \tag{4.54}$$

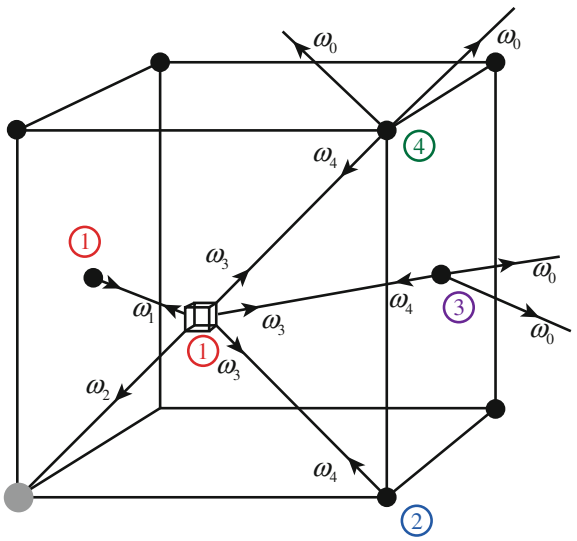

Fig. 4.21 Frequencies ω_j for vacancy-atom jumps in fcc crystals. The *arrows* indicate the direction the vacancy moves. The *circled numbers* indicate the order of neighbors to the solute atom at the origin (after [6])

4.3.6 *Equations for* D

We are now in a position to write the expressions for the diffusion coefficients for the motion of the defects and of the atoms by way of the defects.

1. The vacancy diffusion coefficient is given by:

$$D_{\mathrm{v}} = \alpha a^2 \omega,$$

where

$$\omega = v \exp\left(\frac{-\Delta G_{\mathrm{m}}^{\mathrm{v}}}{k\mathrm{T}}\right) = v \exp\left(\frac{S_{\mathrm{m}}^{\mathrm{v}}}{k}\right) \exp\left(\frac{-E_{\mathrm{m}}^{\mathrm{v}}}{kT}\right),$$

then

$$D_{\mathrm{v}} = \alpha a^2 \omega = \alpha a^2 v \exp\left(\frac{S_{\mathrm{m}}^{\mathrm{v}}}{k}\right) \exp\left(\frac{-E_{\mathrm{m}}^{\mathrm{v}}}{kT}\right). \tag{4.55}$$

2. The vacancy self-diffusion coefficient is the product of the vacancy diffusion coefficient and the probability that the nearest neighbor site is vacant, N_{v}:

$$D_{\mathrm{v}SD} = D_a^{\mathrm{v}} = \alpha a^2 N_{\mathrm{v}} \omega,$$

where

$$N_{\mathrm{v}} = \exp\left(\frac{-\Delta G_{\mathrm{f}}^{\mathrm{v}}}{kT}\right) = \exp\left(\frac{S_{\mathrm{f}}^{\mathrm{v}}}{k}\right) \exp\left(\frac{-E_{\mathrm{f}}^{\mathrm{v}}}{kT}\right),$$

giving

$$D_{\mathrm{vSD}} = D_{\mathrm{a}}^{\mathrm{v}} = \alpha a^2 v \exp\left(\frac{S_{\mathrm{f}}^{\mathrm{v}} + S_{\mathrm{m}}^{\mathrm{v}}}{k}\right) \exp\left(\frac{-E_{\mathrm{f}}^{\mathrm{v}} - E_{\mathrm{m}}^{\mathrm{v}}}{kT}\right). \tag{4.56}$$

3. The interstitial diffusion coefficient is:

$$D_{\mathrm{i}} = \alpha a^2 \omega,$$

or

$$D_{\mathrm{i}} = \alpha a^2 v \exp\left(\frac{S_{\mathrm{m}}^{\mathrm{i}}}{k}\right) \exp\left(\frac{-E_{\mathrm{m}}^{\mathrm{i}}}{kT}\right). \tag{4.57}$$

4. The interstitial self-diffusion coefficient is the interstitial diffusion coefficient times the probability that a neighboring site contains an interstitial, N_i:

$$D_a^i = \alpha a^2 N_i \omega,$$

where

$$N_i = \exp\left(\frac{-\Delta G_f^i}{kT}\right) = \exp\left(\frac{S_f^i}{k}\right)\exp\left(\frac{-E_f^i}{kT}\right),$$

giving

$$D_a^i = \alpha a^2 \nu \exp\left(\frac{S_f^i + S_m^i}{k}\right)\exp\left(\frac{-E_f^i - E_m^i}{kT}\right). \tag{4.58}$$

The diffusion coefficients are all different in detail, but similar in form as they consist of two factors: a constant that is independent of temperature and an exponential of temperature containing an energy term. All equations for D can be rewritten in the form:

$$D = D_0 \exp(-Q/kT), \tag{4.59}$$

where $D_0 = \alpha a^2 \nu$ is the temperature-independent term and Q is the activation energy. For vacancy diffusion, we have:

$$Q_v = E_m^v, \tag{4.60}$$

and for vacancy self-diffusion we have:

$$Q_a^v = E_f^v + E_m^v. \tag{4.61}$$

For interstitials, we have:

$$Q_i = E_m^i, \tag{4.62}$$

and for interstitial self-diffusion, we have:

$$Q_a^i = E_f^i + E_m^i. \tag{4.63}$$

It follows that the activation energy for diffusion of atoms in a crystal depends on both the energy of formation of defects and the energy required for their migration in the periodic field of the crystal lattice. Experiments can be conducted to confirm the temperature dependence of D and also the values of Q. The terms in the pre-exponential factor for the various diffusion mechanisms are provided in Table 4.2 for the fcc and bcc lattices.

Table 4.2 Parameters in the expression for the diffusion coefficient, $D = \alpha a^2 N \omega$, where $\alpha = \frac{1}{6} z A^2$ for the various diffusion mechanisms in the fcc and bcc lattices

Diffusion mechanism	z	A	α	N	D
fcc					
Vacancy	12	$1/\sqrt{2}$	1	1	$a^2\omega$
Vacancy self-diffusion	12	$1/\sqrt{2}$	1	N_V	$a^2 N_v \omega$
Interstitial	12	1/2	1/2	1	$\frac{1}{2}a^2\omega$
Interstitial self-diffusion	12	1/2	1/2	N_i	$\frac{1}{2}a^2 N_i \omega$
bcc					
Vacancy	8	$3/\sqrt{2}$	1	1	$a^2\omega$
Vacancy self-diffusion	8	$3/\sqrt{2}$	1	N_v	$a^2 N_v \omega$
Interstitial	4	1/2	1/6	1	$\frac{1}{6}a^2\omega$
Interstitial self-diffusion	4	1/2	1/6	N_i	$\frac{1}{6}a^2 N_i \omega$

Example 4.3. Determination of D_a^v and D_a^i for fcc copper at 500 °C
For copper:

$$\begin{aligned} E_f^v &= 1.27 \text{ eV}, \quad E_f^i = 2.2 \text{ eV} \\ E_m^v &= 0.8 \text{ eV}, \quad E_m^i = 0.12 \text{ eV} \\ S_f^v &= 2.4k, \quad\quad S_f^i = \sim 0 \end{aligned}$$

and we neglect S_m^v and S_m^i.
For the fcc lattice, $z = 12$, $A = 1/\sqrt{2}$, and $a \sim 0.3$ nm, giving:

$$\begin{aligned} D_v &= \alpha a^2 v \exp\left(\frac{-0.8}{kT}\right) \\ &\cong 5 \times 10^{-6} \text{ cm}^2/\text{s} \\ D_i &= \alpha a^2 v \exp\left(\frac{-0.12}{kT}\right) \\ &\cong 7 \times 10^{-2} \text{ cm}^2/\text{s} \\ D_a^v &= \alpha a^2 v \exp\left(\frac{2.4k}{k}\right) \exp\left(\frac{-1.27 - 0.8}{kT}\right) \\ &\cong 3 \times 10^{-13} \text{ cm}^2/\text{s} \\ D_a^i &= \alpha a^2 v \exp\left(\frac{-2.2 - 0.12}{kT}\right) \\ &\cong 3 \times 10^{-16} \text{ cm}^2/\text{s} \end{aligned}$$

Note that while $D_i/D_v \sim 10^4$ due to the smaller migration energy for interstitials than for vacancies, $D_a^i/D_a^v \sim 10^{-3}$ because of the very high interstitial formation energy compared to that for vacancies. Plots of the

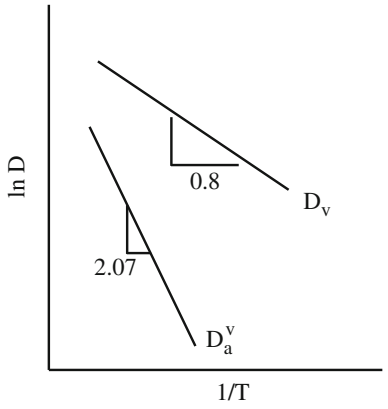

Fig. 4.22 Comparison of plots of ln D versus $1/T$ for vacancy diffusion and vacancy self-diffusion

diffusion coefficients are shown in Fig. 4.22. Note that the vacancy diffusion coefficient is larger than the vacancy self-diffusion coefficient and has a smaller slope.

The behavior of self-interstitial atoms in bcc iron at 323 °C is illustrated in Movie 4.3 (http://rmsbook2ed.engin.umich.edu/movies/). In this movie, the green balls are the interstitials and the red ball is the vacant lattice site, and together they form a SIA dumbbell in which the two green atoms share a single lattice site. The SIA originates as a ⟨110⟩ split-dumbbell interstitial and then rotates into a ⟨111⟩ interstitial and moves in one-dimension through the ⟨111⟩ crowdion saddle position. Movie 4.4 shows a di-SIA consisting of two parallel ⟨111⟩ split-dumbbells that migrates along the ⟨111⟩ direction and also rotates to different ⟨111⟩-type orientations.

4.4 Correlated Diffusion

Earlier we assumed that irrespective of the kinds of defects present in a crystal lattice, successive jumps of atoms are completely random or uncorrelated. This means that after n jumps, all possible directions for the $(n + 1)$th jump are equally probable. This is true for vacancies or interstitials since all structural elements surrounding them are at all times identical. Since the vibrational frequency of a lattice atom is several orders of magnitude greater than the jump frequency, equilibrium in the region surrounding the defect is rapidly established between successive jumps and the next jump occurs with no effect of the previous jump on its direction. But this does not always hold true for atom diffusion as described in [5] and in the following.

If we consider the case of a radioactive tracer to track atom diffusion, a tracer will make a jump if a vacancy is in its immediate vicinity. The second jump is uncorrelated with the first if the probability of the second jump is the same for all directions. However, the tracer arrives from a position that is vacant at the time of its arrival. Hence, when it is "preparing" for the next jump, the chance that the position from which it has arrived is unoccupied is greater than for any other position around the atom. The two jumps are correlated since the probability of the tracer returning to its former position is higher than for making a jump in any other direction. In other words, the tracer has a greater tendency to move in the direction from which it came than in the direction it is headed, or from Eq. (4.35), $\overline{\cos\theta_2} < 0$.

Since jumps in the direction from which it came are most probable, the tracer will have traveled a shorter (net) distance than that traveled by the vacancy. Therefore, the self-diffusion coefficient of the tracer (which is a measure of the rate of this process) is smaller than that of the atoms constituting the lattice, since the self-diffusion of the tracer is a correlated random walk, whereas the movement of the vacancies and consequently of the atoms constituting the lattice are not correlated.

The correlation effect is absent in the simple interstitial mechanism, but there is correlation of motion by the interstitialcy mechanism. In both, the vacancy and the interstitialcy mechanisms, $D_{\text{tracer}} < D_{\text{lattice}}$, and:

$$f = \frac{D_{\text{tracer}}}{D_{\text{lattice}}}, \tag{4.64}$$

and f is known as the *Haven coefficient* and is a measure of the degree to which diffusion is random. Recall our earlier discussion of the measurement of the square of the displacement by random walk given by Eq. (4.35):

$$r^2 = n\lambda^2\left(1 + \frac{2}{n}\sum_{i=1}^{n-1}\sum_{j\neq i}^{n}\cos\theta_{ij}\right),$$

where the mean square displacement is obtained by averaging over all values of $\cos\theta_{ij}$. In this expression, the term in brackets is f and the value of f for random walk is 1 since the average over all $\cos\theta_{ij}$ is 0. But when there is correlation between successive jumps, f is $\neq 1$. For the vacancy mechanism of diffusion of a tracer in a regular lattice [5]:

$$f_{\text{v}} = \frac{1 + \overline{\cos\theta}}{1 - \overline{\cos\theta}}, \tag{4.65}$$

and for interstitial diffusion,

$$f_i = 1 + \overline{\cos\theta}. \tag{4.66}$$

Since in both cases, $\overline{\cos\theta} < 0$, then $f < 1$.

A simpler treatment of f_v is that $f_v = \dfrac{1-P}{1+P}$, where P is the probability of a jump of a tracer to a neighboring vacancy, and $1 - P$ is the probability that a neighboring vacancy will move away as a result of jumps of lattice atoms. To a first approximation, P is equal to the reciprocal of the number of nearest lattice sites, z, around the tracer. Therefore:

$$f = \frac{1-1/z}{1+1/z} = \frac{z-1}{z+1}. \tag{4.67}$$

For the fcc lattice:

$$f = \frac{1-1/12}{1+1/12} = \frac{12-1}{12+1} = 0.85.$$

For the bcc lattice:

$$f = \frac{1-1/8}{1+1/8} = \frac{8-1}{8+1} = 0.78.$$

For the simple cubic (sc) lattice:

$$f = \frac{1-1/6}{1+1/6} = \frac{6-1}{6+1} = 0.71.$$

So, in our microscopic description of the diffusion coefficient, D, Eq. (4.44), we account for correlated diffusion by including the correlation coefficient:

$$D = 1/6 f \lambda^2 \Gamma = f \alpha a^2 \omega. \tag{4.68}$$

As an aside, the true correlation coefficient, f, actually consists of two terms, f' and f'' such that $f = f'\,f''$. The quantity f'' was described in the previous paragraph (as f) and f' is related to the difference between the distances traveled during the elementary act by the tracer atom and the defect:

$$f' = \frac{\lambda_{\text{tracer}}}{\lambda_{\text{defect}}}. \tag{4.69}$$

In the case of a vacancy, $f' = 1$ since $\lambda_{\text{tracer}} = \lambda_{\text{vacancy}}$, or the distance traveled by the tracer and the defect are equal in one jump. The same is true for the simple interstitial mechanism. But in the case of the interstitialcy mechanism, the tracer

Table 4.3 Correlation coefficients for the most common diffusion mechanisms in the various crystal lattices (from [5])

Crystal lattice	Diffusion mechanism	Correlation factor
Simple cubic	Vacancy	0.65311
	Interstitial	
	Collinear	0.80000
	Non-collinear	0.96970
Face-centered cubic	Vacancy	0.72722
	Interstitial	
	Collinear	0.66666
	Non-collinear	0.72740
Body-centered cubic	Vacancy	0.72722
Hexagonal close-packed	Vacancy	0.78121

moves from an interstitial position to a lattice site (or vice versa). In both cases, it travels a distance λ_{tracer}. However, the passage of a lattice atom from an interstitial position to a lattice site is equivalent to the appearance of an identical atom displaced from the lattice site in a neighboring interstitial position. Therefore, the jump of a lattice atom from the interstitial position to a lattice site requires (for the collinear case) a displacement of the lattice atom by a distance $2\lambda_{\text{tracer}}$, or $f' = \lambda_{\text{tracer}}/2\lambda_{\text{tracer}} = 0.5$. For the non-collinear case, $f' = \lambda_{\text{tracer}}/6\lambda_{\text{tracer}} = 2/3$. Table 4.3 summarizes the correlation coefficient for various diffusion mechanisms in the common crystal lattices.

4.5 Diffusion in Multicomponent Systems

Our discussion on diffusion so far has applied only to pure or single-component systems. We have not accounted for multiple components such as impurities in a pure metals and alloys. Diffusion in these systems was treated in experiments conducted by Smigelskas and Kirkendall in 1947 [7] and analyzed by Darken in 1948 [8]. The result is that the diffusion coefficients of the two components in a binary (A–B) system can be expressed as:

$$\tilde{D} = D_{\text{A}} N_{\text{B}} + D_{\text{B}} N_{\text{A}}, \tag{4.70}$$

where $D_{\text{A,B}}$ are the intrinsic diffusion coefficients and are functions of composition, and $\tilde{D}$ is the interdiffusion coefficient. Since the partial diffusion coefficients depend on the alloy composition, $\tilde{D}$ is a complex, nonlinear function of concentration. However, in the case of dilute solutions ($N_{\text{B}} \rightarrow 0$, $N_{\text{A}} \rightarrow 1$), the interdiffusion coefficient is approximately equal to the partial diffusion coefficient of the solute.

The significance of this result can be appreciated by a brief review of the elegance and implications of the experiment. In Kirkendall's experiment,

molybdenum wires were wound around a block of brass (70Cu–30Zn) which was then plated with a thick coating of copper. The molybdenum wires are insoluble in copper and act as inert markers to locate the original interface. When the assembly is heated in a furnace, the wire markers on opposite sides of the brass moved toward each other, indicating that more material has left the brass than entered it, implying that the diffusion coefficient of zinc is greater than that of copper.

The vacancy mechanism is the only diffusion mechanism that can account for marker motion. If zinc diffuses by a vacancy mechanism, then the flux of zinc atoms in one direction must equal the flux of vacancies in the opposite direction and the number of zinc atoms leaving the brass is balanced by an equal number of vacancies entering the brass. But the vacancies are absorbed by internal sinks, so the result is that the volume of the brass diminishes and the markers move closer together. The concept of a flux of atoms giving rise to a flux of defects will be explored in depth in Chap. 6 on Radiation-Induced Segregation, which occurs by the *inverse* Kirkendall effect.

4.6 Diffusion Along High-Diffusivity Paths

Metals and alloys used as structural engineering materials are polycrystals and are thus, inhomogeneous, as they contain grain boundaries, dislocations, internal interfaces due to precipitates or second phases, etc. To understand diffusion in these systems, we must discuss the effect of these linear, planar and area defects on the diffusion process. The primary difference between mono- and polycrystals is that the latter consists of aggregates of crystals oriented (generally) at random. This latter type of structure rarely shows anisotropy of diffusion. The important difference is that linear and planar defects represent high-diffusivity paths along which diffusion can occur much faster than via point defects (bulk diffusion).

Grain boundaries are important high-diffusivity paths since the atom packing density is lower. There exist several models of grain boundary diffusion, and all assume that the boundary has a width, $\delta \sim 0.3–0.5$ nm. One model that is based on the dislocation model of grain boundaries deserves special attention. In this model, the grain boundary is regarded as a number of edge dislocations. The dislocation density (#/unit length) increases with increasing misorientation angle, θ, between two grains in contact (Fig. 4.23). From the figure:

$$d \sin\frac{\theta}{2} = \frac{b}{2}. \tag{4.71}$$

Hence, the distance between neighboring dislocations decreases with increasing misorientation angle. A low-angle grain boundary consisting of many edge dislocations can be regarded as a row of parallel channels in which packing of atoms is loosest. In this region, the strain is high and the packing of atoms is loose, and the diffusion coefficient will be the highest along the dislocation lines (cores).

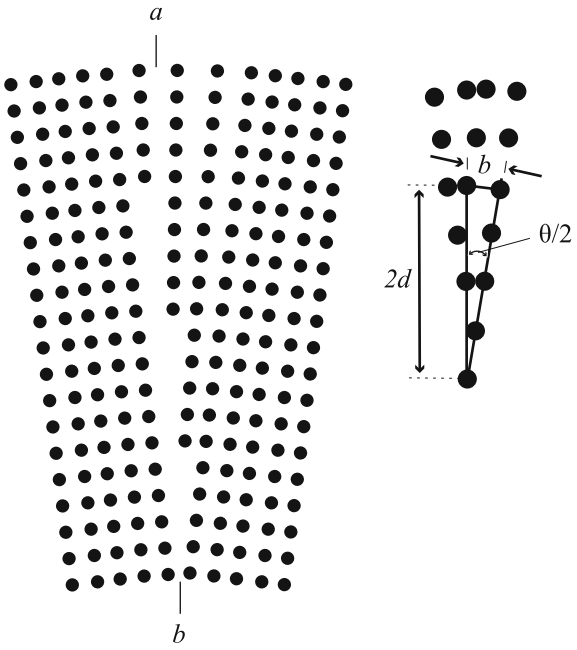

Fig. 4.23 Dislocation model of a small-angle grain boundary and the geometrical relationship between the angle of tilt, θ, the Burgers vector, b, and the spacing between the dislocations, d

According to this model, diffusion along grain boundaries should be anisotropic and depends on the angle θ. The grain boundary described as a slab of uniform thick δ, and diffusion coefficient D_{gb} can also be viewed as a planar array of pipes of radius p and spacing d. Grain boundary diffusion is related to diffusion along dislocation cores (also known as *pipe diffusion*), described by D_p, by the following relation:

$$D_{gb}\delta = D_p\left(\pi p^2/d\right), \tag{4.72}$$

and substituting for d from Eq. (4.71) gives:

$$\begin{aligned} &= D_p \pi p^2 \left(\frac{2\ \sin\theta/2}{b}\right) \\ &\cong \frac{D_p \pi p^2 \theta}{b}. \end{aligned} \tag{4.73}$$

The dislocation model of the grain boundary shown in Fig. 4.23 is expanded in Fig. 4.24 to show that the extra half-planes of atoms can be regarded as edge dislocations. In fact, the rate of diffusion along the grain boundary increases with increasing misorientation angle, θ, and reaches a maximum at $\theta = 45°$ (Fig. 4.25). At angles greater than 45°, the dislocation model of grain boundaries breaks down since the distance between dislocations, d, would have to be smaller than the lattice constant.

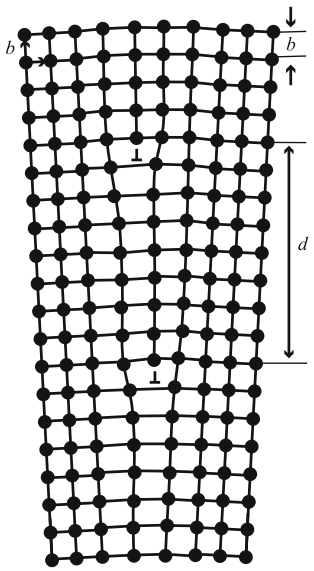

Fig. 4.24 Expanded view of the dislocation model of the grain boundary shown in Fig. 4.23

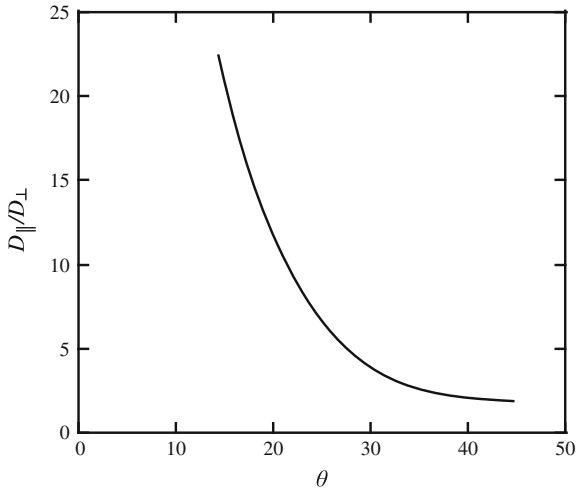

Fig. 4.25 Effect of grain boundary misorientation angle on the diffusion of atoms along grain boundaries (after [5])

This result also indicates that there should be a relationship between the mean value of the diffusion coefficient, $\bar{D}$, in a polycrystalline material and the grain size, d, since as the grain size decreases, the grain boundary area per unit volume increases. Therefore, $\bar{D}$ should increase with decreasing grain size as shown in Fig. 4.26. We can write the diffusion coefficient of a solid in which diffusion occurs by bulk diffusion (vacancy mechanism) and grain boundary diffusion as:

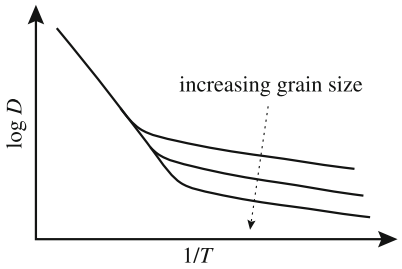

Fig. 4.26 The effect of grain size on the character of diffusion in polycrystalline solids

$$\bar{D} = D_a^v \exp\left(\frac{-Q_a^v}{kT}\right) + D_{gb} \exp\left(\frac{-Q_{gb}}{kT}\right), \tag{4.74}$$

where D_a^v and Q_a^v refer to vacancy self-diffusion, and D_{gb} and Q_{gb} refer to grain boundary diffusion. In most metals, $Q_a^v \sim 2Q_{gb}$, so at low temperature, grain boundary diffusion dominates and at high temperature, diffusion is dominated by bulk, or volume diffusion (Fig. 4.26).

Pipe diffusion along dislocation cores can also influence low temperature lattice diffusion and the total diffusion coefficient can be estimated simply by:

$$\bar{D} = gD_p + (1-g)D_a^v, \tag{4.75}$$

where $\bar{D}$ is the mean diffusion coefficient, D_p is the diffusion coefficient for dislocations and D_a^v is the self-diffusion coefficient, and g is the fraction of time that the diffusing atom spends within the dislocation. As the dislocation density increases, g increases, and since $D_p > D_a^v$, then $\bar{D}$ increases as well.

This general formulation can also be applied to interface or surface diffusion occurring on internal and external surfaces of solids. In general, for defects in the lattice, the more loosely bound the atoms, the lower is the activation energy and the higher is the diffusion coefficient. So surface diffusion requires a lower activation energy than for other forms of diffusion since each surface atom has only half the nearest neighbors as it does in the bulk, and generally:

$$Q_{surface} < Q_{gb} < Q_p < Q_a^v, \quad \text{and so} \quad D_{surface} > D_{gb} > D_p > D_a^v. \tag{4.76}$$

Nomenclature

a	Lattice constant
A	Factor depending on geometry and diffusion mechanism
C	Concentration
D_x^y	Diffusion coefficient of species x via y
D_{gb}	Diffusion coefficient for grain boundary diffusion

$\tilde{D}$ Interdiffusion coefficient
$\bar{D}$ Mean value of diffusion coefficient in a polycrystalline material
D_{lattice} Diffusion coefficient of lattice atom
D_{p} Diffusion coefficient for pipe diffusion
D_{tracer} Diffusion coefficient of tracer atom
E Energy
f Correlation (Haven) coefficient
F Helmholtz free energy
g Fraction of time a diffusing specie spends within a dislocation
G Gibbs free energy
H Enthalpy
J Flux [cm^{-2}]
k Boltzmann's constant
n Number of defects
n_{m} Number of activated complexes
N Number of sites
p_{v} Probability that a lattice site is vacant
P Pressure, also probability
Q Activation energy
R Radius
r_{a} Radius of an atom
S Entropy
T Temperature
U Internal energy
V Volume
z Number of nearest neighbors
α $\frac{1}{6}zA^2$
δ Width of the barrier in an activated complex, also grain boundary width
γ Stacking fault energy
Γ Jump frequency
κ_{r} Thermal conductivity
Λ Jump distance
μ Shear modulus
ν Frequency, also Poisson's ratio
ν_{E} Natural frequency of an oscillator
ν_{r} Perturbed frequency of an oscillator
σ Surface energy
$\bar{v}$ Average velocity of atoms moving through barrier in activated complex, Eq. (4.50)
ω Jump frequency to a single site
Ω Volume of an atom

Subscripts

a Atom
E Natural contribution to v
f Formation
gb Grain boundary
i,v Interstitials, vacancies
m Migration
p Pipe
r Vibrational contribution to v
th Thermal

Superscripts

FP Frenkel pair
i,v Interstitials, vacancies
mix Mixing

Acronyms

SIA Single interstitial atom

Problems

4.1 Many metals occur with both bcc and fcc structure, and it is observed that the transition from one structure to the other involves only insignificant volume change. Assuming *no* volume change, find the ratio D_{fcc}/D_{bcc} where D_{fcc} and D_{bcc} are the closest distances between metal atoms in the respective structures.

4.2 For a Ni lattice, calculate the following parameters for atomic chains along the (110) direction:

(a) the number of atoms per unit chain length,
(b) the number of chains per unit area, and
(c) the product of the two. What is this product?

4.3 In the past, investigators have sometimes considered an interstitial atom as having been produced by the transfer of an atom from a normal lattice site to an interstitial site, thus resulting in a one-to-one correspondence between the concentrations of vacancies and interstitials. However, the equilibrium number of vacancies is generally orders of magnitude greater than the equilibrium number of interstitials at a given temperature. Explain.

4.4 The magnitude of the relaxation volume, $|V|$, is greater than 1.0 for interstitials and is less than 1.0 for vacancies. Explain.

4.5 In terms of the jump frequency to a particular neighboring site, ω, and the lattice constant, a, what is the diffusion coefficient for impurity atoms whose equilibrium position is the octahedral interstitial site in:

(a) the fcc lattice?
(b) the bcc lattice?

4.6 Consider a rigid crystal in the shape of a sphere of radius R. We create a small cavity of radius r (one atomic volume) in the center of the sphere. The material that was in this volume is spread uniformly over the surface of the sphere (assuming this can be done), increasing the radius of the sphere to R'.

(a) Show that for an atomic radius of 0.15 nm and an intrinsic surface energy, $\sigma \sim 10$ eV/nm^2, the formation energy of a vacancy is of order $\simeq$2 eV
(b) If instead of a rigid solid, the crystal is treated as an elastic continuum, how would this affect the value of E_f^v you calculated for part (a)? Why?

4.7 Calculate the diffusion coefficients for interstitials and vacancies in copper at 484 °C. Neglect the contributions of mixing entropy. Use 0.361 nm for the lattice constant. Also, calculate the vacancy self-diffusion coefficient. Why is this so much lower than the diffusion coefficients for vacancies?

4.8 In a laboratory experiment conducted at 10 °C below the melting point of copper, 0.02 % of the atom sites are vacant. At 500 °C, the vacant atom fraction was 5.7×10^{-8}.

(a) What is the vacancy formation energy?
(b) How many vacancies are there per cm^3 at 800 °C?

4.9 For the case in Problem 4.7, determine the thermal equilibrium concentrations of vacancies and interstitials.

References

1. Ullmaier H, Schilling W (1980) Radiation damage in metallic reactor materials. In: Physics of modern materials, (vol. 1). IAEA, Vienna
2. Hackett MJ, Was GS, Simonen EP (2005). J ASTM Int 2(7)
3. Thompson MW (1969) Defects and radiation damage in metals. Cambridge University Press, Cambridge
4. Shewmon PG (1989) Diffusion in solids. The Minerals, Metals and Materials Society, PA
5. Mrowec S (1980) Defects and diffusion in solids, an introduction. Elsevier, New York
6. LeClaire AD (1978) J Nucl Mater 69–70:70
7. Smigelskas A, Kirkendall E (1947) Trans AIME 171:130
8. Darken L (1948). Trans AIME 175:184–201